Acta Radiologica Oncology 22 (1983) Fasc. 3

FROM THE DEPARTMENT OF HOSPITAL PHYSICS, KAROLINSKA SJUKHUSET, S-10401 STOCKHOLM, SWEDEN.

NON-UNIFORMITY INDUCED ARTIFACTS IN SINGLE-PHOTON EMISSION COMPUTED TOMOGRAPHY

B. AXELSSON, A. ISRAELSSON and S. LARSSON

Emission computed tomography (ECT) with rotating gamma cameras is being increasingly used for nuclear medicine examinations. The diagnostic accuracy of the technique has been found to be superior to conventional scintigraphy for several applications (BERGSTEDT et coll. 1981, BIERSACK et coll. 1982, GO et coll. 1982) but might, however, be impaired due to image artifacts. For example, the contrast enhancement achieved with the technique will impose high demands on the gamma camera as regards uniform response over the entire detector surface (LARSSON 1980, SOUSSALINE et coll. 1981). A deviation from uniformity in the field of view of the camera will introduce an error in the same position in the projection data in each view, i.e. a systematic bad ray, which will cause ring artifacts in the reconstructed image (SHEPP & STEIN 1977, KOWALSKI 1977).

Previous reports on the uniformity of gamma cameras have mostly dealt with reasonable demands for conventional scintigraphy (COHEN et coll. 1976, HASMAN et coll. 1976, TODD-POKROPEK et coll. 1977, MUEHLLEHNER et coll. 1981). Modern gamma cameras without on-line correction have a non-uniformity below ~5 per cent (rms) within the useful field of view and this is mostly regarded as satisfactory for conventional scintigraphy. However, for ECT it may not be sufficient in order to obtain accurate results.

Therefore the abundance and magnitude of artifacts appearing in the reconstructed images due to uniformity defects in the field of view of the gamma camera were investigated. The transfer of defects from projection data to the reconstructed image has been analysed by means of computer simulations. Changes of uniformity due to various factors such as choice of flood source configuration and camera head orientation, and their influence on the reconstructed image, have been evaluated from phantom measurements. The equipment used was a GE 400 T gamma camera operating with the SPETS-system for ECT (LARSSON). The results obtained have been used to design a uniformity correction technique that will greatly reduce the non-uniformity induced artifacts in the reconstructed image.

Computer simulations

A deviation from uniformity in the field of view of the gamma camera disturbs the projection data in the same position in each angle of the acquisition investigation (a 'systematic bad ray'). The origin of systematic deviations in the projection data is mainly twofold: (a) mainly low frequency variations due to non-linearity and sensitivity variations in the field of view of the gamma camera, and (b) high frequency variations induced by statistical uncertainties in the conventional inverse flood field matrices used for non-uniformity correction. Even small errors introduced from statistical uncertainties might be of importance due to the enhancement of high frequency components in ECT (ROGERS et coll. 1982).

Accepted for publication 9 December 1982.

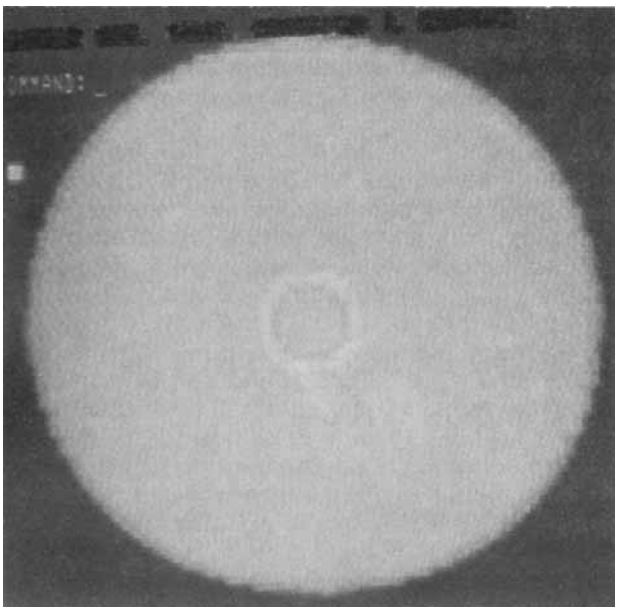

Fig. 1

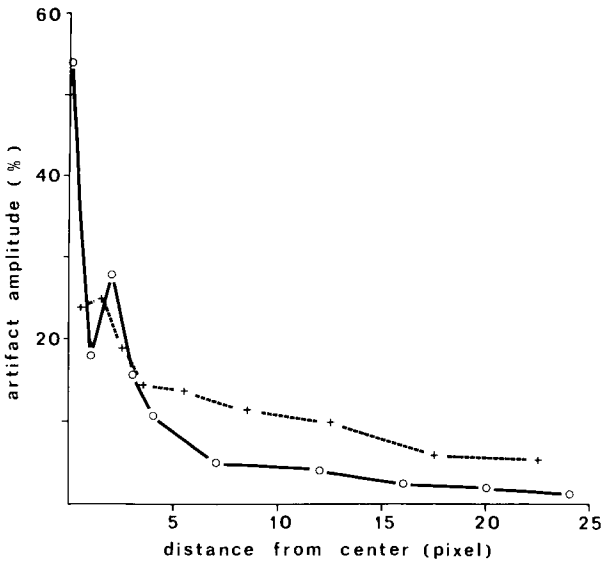

Fig. 2a

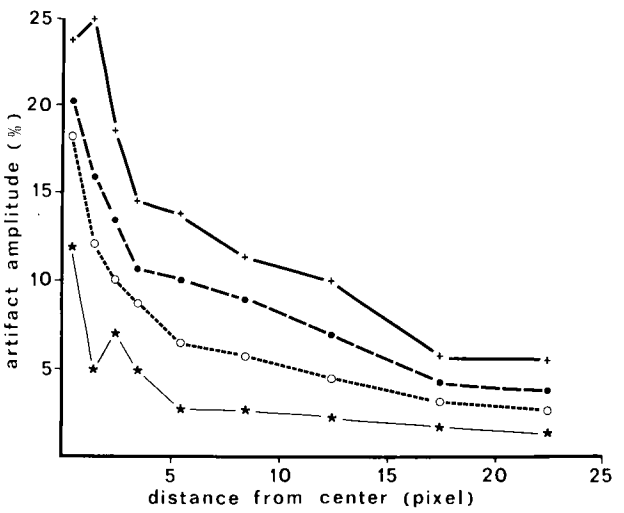

Fig. 2b

Fig. 1. Image reconstructed from simulated data. Simulated projection data contained 2 per cent defect, one pixel wide, 4 pixels from center of rotation.

Fig. 2. Artifact amplitude in the reconstructed image for a defect in projection data at different distances from the center of rotation. a) Defects one (+—+) and two (○—○) pixels wide ramp filter and nearest value interpolation, b) defect one pixel wide; (+—+) ramp filter nearest value interpolation; (●—●) filter 2, nearest value, interpolation; (○—○) filter 2, linear interpolation; (x—x) filter 5, nearest value interpolation.

Systematic bad ray. The transfer of small defects from projection data to the reconstructed image was examined from computer simulations of ideal data from a cylindric object with 30 pixel radius corresponding to a real object radius of 18 cm. The same projection data were used for all 64 angles in the reconstruction. The simulations did not consider effects of scatter, attenuation etc., i.e. a numeric analysis of the artifact enhancement by the reconstruction technique. The reconstructions were performed using the ramp filter with nearest value interpolation. Positive defects of 2 per cent of the ideal data, one and two pixels wide, respectively, were introduced in the projection data at different distances from the center of rotation. An example of the reconstructed images is presented in Fig. 1. The maximum artifact was evaluated as the maximum deviation (positive or negative) from the mean since a positive defect in the projection data will create both positive and negative ring artifacts in the reconstructed image (cf. Fig. 1). The magnitude of the artifact increases as the defect in projection data is introduced closer to the center of rotation (Fig. 2a). A 2 per cent defect two pixels wide at the center of rotation will introduce an artifact of 54 per cent in the reconstructed image while a defect one pixel wide will give an artifact with about half that magnitude (25%). The smaller magnitude of the latter

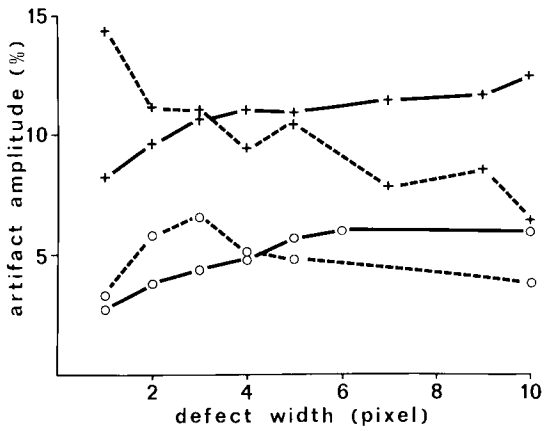

Fig. 3. Amplitude of positive (---) and negative (—) artifact in the reconstructed image for different width of a + 2 per cent defect in projection data. Images reconstructed with ramp filter (+) and filter 5 (○).

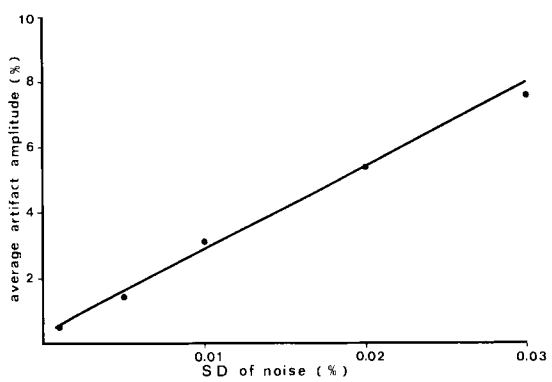

Fig. 4. Average artifact amplitude in the reconstructed image as a function of noise level in simulated projection data.

Table 1

Average artifact amplitude with different concentration ratio inside and outside cylinder

Concentration ratio	Average artifact amplitude (%)
1/1	51
1/0.5	35
1/0.25	29
1/0.13	19
1/0	14

artifact is due to addition of opposed projections before reconstruction (the arithmetic mean). Since the center of rotation is defined to correspond to the location between pixel 32 and 33 the defect will be positioned in pixel 32 in one view and pixel 33 in the opposing view. Therefore a defect (two pixels wide) located in pixels 32 and 33 represents the 'worst case'. For lager distances r, from the center of rotation the magnitude of the artifact is reduced approximately as $r^{-1/2}$ with distance in accordance with theory (SHEPP & STEIN).

The use of more smoothing filters, as well as linear interpolation instead of nearest value interpolation will reduce the magnitude of the artifacts (Fig. 2 b). The filters used are the ramp filter and modified versions of the filter proposed by SHEPP & LOGAN (1974). For $\nu \leq \nu_c = (2\ a)^{-1}$ the different filters have the following expressions:

Filter 0 (ramp filter)

$$\varphi\ (\nu) = |\nu|$$

Filter 2

$$\varphi(\nu) = (0.9+0.1\ \cos\ 2\pi a\nu) \left| \frac{\sin\ \pi\nu a}{\pi a} \right|$$

Filter 5

$$\varphi(\nu) = (0.4+0.6\ \cos\ 2\pi a\nu) \left| \frac{\sin\ \pi\nu a}{\pi a} \right|$$

while all filters $\varphi(\nu)=0$ for $\nu>\nu_c$

where ν is the frequency and a is the sampling distance. The influence from width and shape of the deviations in the projection data was examined by introduction of a positive defect (2%) in the projection data, with the inner limit of the defect 4 pixels (25 mm) from the center of rotation and with defect widths from 1 to 10 pixels. The results are presented in Fig. 3. Though the positive artifact magnitude is reduced as the defect width is increased, the negative artifact magnitude is increased. The effect of increased defect width on the maximum artifact magnitude is therefore not marked. The reduction of artifact magnitude for very small defect widths and using the most smoothing filter function is due to insufficient build-up.

Uniformity defects that are not caused by statistical uncertainties in the inverse flood field correction matrix usually exhibit rather smooth variations. This was simulated by a Gaussian shaped defect in the projection data. The center of the defect was located 6 pixels from the center of rotation. The maximum amplitude was 2 per cent and the width (FWHM) was 6 pixels. The artifact magnitude in the reconstructed image was 5 per cent if filter 2 was used. The artifact magnitude for a 'square wave' defect (2% defect, 6 pixels wide, center of defect 6 pixels from center of rotation) was 9 per cent. The increased artifact magnitude in the latter case is due to the enhancement of high frequency components in the reconstruction.

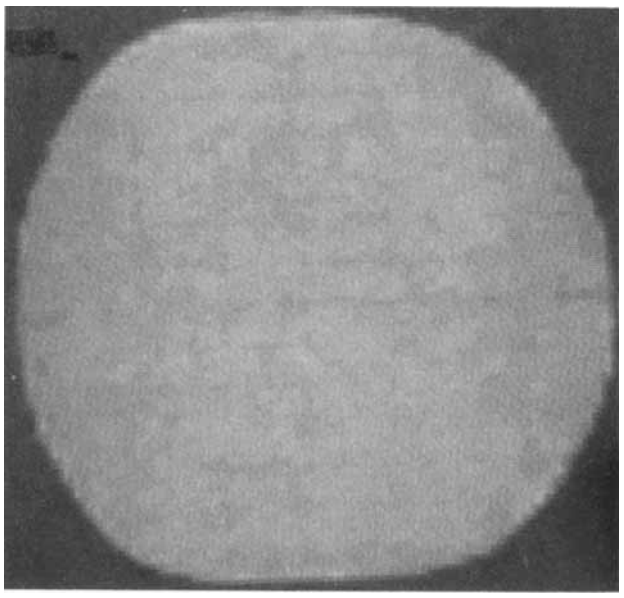

Fig. 5

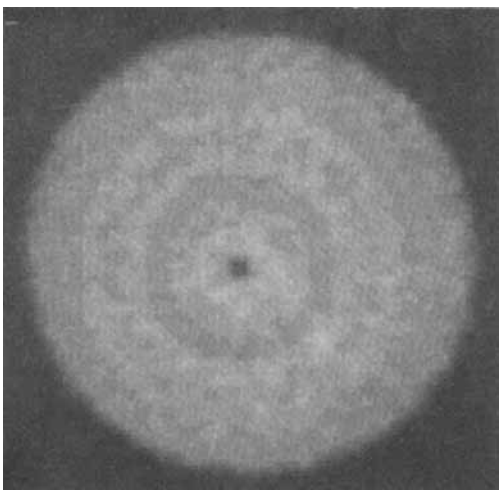

Fig. 6a

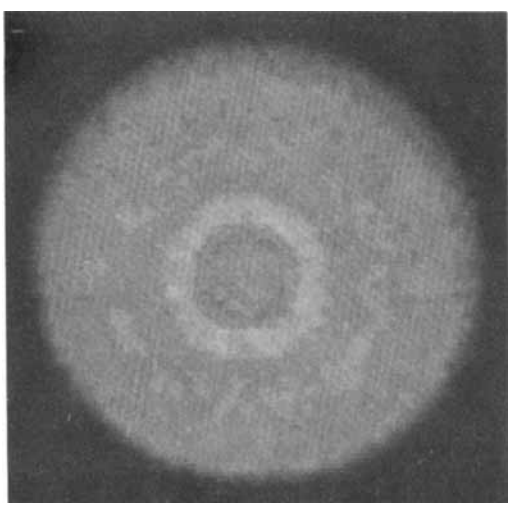

Fig. 6b

Fig. 5. Flood field image obtained with ^{57}Co flood source and 50 mm of polystyrene between flood source and low energy general purpose collimator.

Fig. 6. Example of reconstructed images from phantom. a) Section with largest negative artifact, b) section with largest positive artifact.

Object size. The magnitude of the artifacts in the reconstructed image is proportional to the number of sampling points per slice in each view (SHEPP & STEIN). This also applies to the size of the object containing radionuclide. Computer simulations with different object diameters show that the artifact magnitude decreases in proportion to the decrease in object diameter. These simulations, however, deal with an ideal situation with uniform activity inside the object and no activity outside the object. The influence on artifact magnitude from activity outside a small object was investigated using phantom measurements. A cylinder with 100 mm diameter was positioned inside at the center of a larger cylindric phantom with 300 mm diameter. The ratio of the activity concentration inside and outside the smaller phantom was varied and the magnitude of ring artifacts close to the center of rotation in the reconstructed sections were evaluated. The results are presented in Table 1.

The table gives the average artifact amplitude, for different concentration ratios. The average artifact amplitude increases approximately in proportion to the increased activity concentration in the large object. When the activity concentration ratio is 1/1, which corresponds to an object of 300 mm diameter, the average artifact amplitude is ~3.5 times the average artifact amplitude with activity only in the small object (∅=100 mm). This agrees reasonably well with theory as mentioned.

Statistical accuracy of non-uniformity correction matrix. When non-uniformity correction is per-

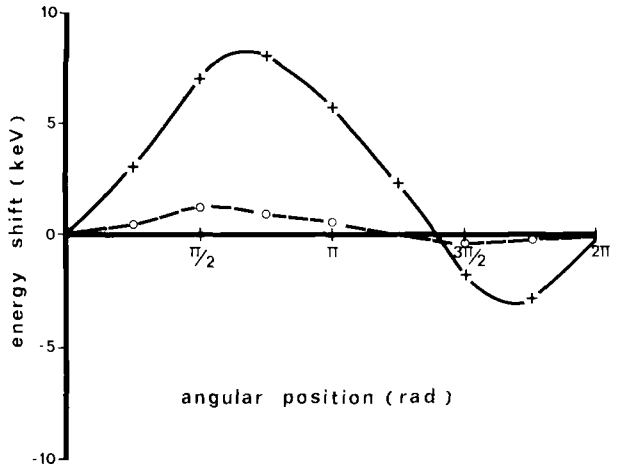

Fig. 7. Energy shift in PM tube signal registered at the center of the gamma camera with the camera in different angular positions, (+—+) without μ-metal shields, (○—○) with μ-metal shields.

Table 2

Flood field images compared with flood field image obtained with ^{57}Co flood source

	Flood source		
	^{57}Co + scatter	$^{99}Tc^{m}$	$^{99}Tc^{m}$ + scatter
Percentage of pixels deviating more than ±3 SD	7.0	14.4	19.0
Maximum deviation (%)	12.6	24.2	33.6

formed using multiplication with an inverse flood field matrix. The accuracy of the correction factors depend i.a. on the number of counts accumulated per pixel. Poor statistical accuracy will introduce one-pixel defects, corresponding to a systematic bad ray, in the projection data as described (GULLBERG et coll. 1982, NOWAK et coll. 1982). In order to simulate the appearance of artifacts in the reconstructed image from the uncertainty due to counting statistics in the inverse flood field matrix, noise was introduced in the ideal projection data. The standard deviation (SD) of the Gaussian distributed noise was varied between 0.1 and 3 per cent and 10 sections were reconstructed, using filter 2, for each noise level. The average error (rms) in the reconstructed sections as a function of the noise level is presented in Fig. 4. In order to achieve an average artifact amplitude in the reconstructed sections of less than 3 per cent rms (which is the same level of non-uniformity as when this equipment is used for conventional scintigraphy) more than 10000 counts/pixel (SD of 1%) should be acquired for the inverse flood field matrix (total of ~30 Mcounts).

However, because of statistics, an SD of 1 per cent implies a probability that the maximum defect will be 3 per cent and as can be deducted from Fig. 2 a one pixel wide defect in the projection data with an amplitude of 3 per cent will, when appearing close to the center of rotation, introduce an artifact of ~35 per cent in the reconstructed image. Therefore, to reduce the possibility of disturbing ring artifacts close to the center of rotation in the reconstructed images it is desirable to accumulate at least 100000 counts/pixel in the inverse flood field matrix. This will result in an average error due to statistics of ~0.3 per cent (SD) and a 0.3 per cent defect at the center of rotation will introduce an artifact of 4 per cent in the reconstructed image. This is, however, not always possible, due to limited word length of the matrix, neither for the present uniformity corrector of the GE 400T (12 bit memory word, maximum of 4026 counts/pixel) nor for the GAMMA 11 correction matrix (16 bit memory word, maximum of 65535 counts/pixel). A smoothing of the inverse flood field matrix to achieve a reduction of the statistical uncertainty might introduce systematic artifacts if the acquisition investigation not is smoothed in the same way (ROGERS et coll.). Smoothing will, however, degrade the resolution in the reconstructed sections.

Measurements

Abundance and magnitude of artifacts. The measurements were performed with a GE 400T camera, operating with the SPETS-system for ECT (LARSSON). The camera is supplied with a 64×64 12 bit word on-line non-uniformity corrector and the PM-tubes (37) were individually shielded by μ-metal.

The correction matrix was acquired using a ^{57}Co flood source, and the uniformity corrector was in operation in all measurements. The uniformity of the field of view of the gamma camera was investigated using a conventional ^{57}Co flood source and 50 mm of polystyrene between the flood source and the LEGP (low energy general purpose) collimator (Fig. 5). No obvious non-uniformity defects were found within the useful field of view. The rms error within a diameter of 300 mm was ±3 per cent.

Non-uniformity induced artifacts in reconstructed

images were analysed by phantom measurements. The phantom used was a plexiglass cylinder with diameter 300 mm and length 150 mm filled with a uniform solution of $^{99}Tc^{m}$. The central axis of the phantom was positioned approximately at the center of rotation and ECT was performed using the same technique as is used in clinical examinations. The acquisition time was chosen to assure an average of 4 Mcounts per angle in the 64 angle investigation. Some examples of the images obtained are shown in Fig. 6. The section with the largest 'negative' artifact (−54% compared with average within image) is shown in Fig. 6a and the section with largest 'positive' artifact (+31%) in Fig. 6b. Ring artifacts were present in all reconstructed sections and the average rms error within a diameter of 250 mm in 10 reconstructed sections was ±8 per cent.

Flood field sources. The pitfalls in using multiplication with an inverse flood field matrix for non-uniformity correction has been discussed previously (PADIKAL et coll. 1976, LEWIS et coll. 1978, WICKS et coll. 1979, PITT et coll. 1981). It is evident that the non-uniformity depends on the choice of flood source. The differences between flood-field matrices obtained from different flood field sources with this gamma camera were analysed using ^{57}Co and $^{99}Tc^{m}$ flood sources with and without 5 cm of polystyrene between the source and the collimator.

The $^{99}Tc^{m}$ flood source used has a polystyrene body 470 mm × 470 mm with a 435 mm diameter cavity for the nuclide. The distance between the 5 mm thick plexiglass walls is 13 mm. The flood source was clamped between flat plates during filling to avoid bulging.

Approximately 10000 counts/cell (64×64 matrix) were acquired for each of the flood fields used. All flood field images were normalized to the same number of average counts/cell and compared with the flood field obtained when the ^{57}Co flood source was positioned directly on the collimator. The comparisons were performed pixel by pixel, for each cell within 250 mm diameter and the number of pixels deviating more than ±3 SD were recorded. The results are presented in Table 2 together with the maximum deviation recorded. Non-uniformity changes were substantial in all cases. Since very small changes in uniformity are to be detected the uniformity of the ^{57}Co flood source should be evaluated (if such a source is used to obtain flood field images) or care should be taken to have the flood source in exactly the same position in each measurement if the results from different measurements are to be compared.

Table 3

Flood field images with gamma camera in different angular positions compared with flood field image obtained with camera in angular position 180°

	Angular position (degrees)			
	0	90	200	270
Percentage of pixels deviating more than ±3 SD	6.4	2.1	1.2	1.7
Maximum deviation (%)	8.0	5.8	6.0	6.8

Table 4

Flood field images obtained at different time intervals compared with flood field image obtained at time interval 0 to 80 min

Time interval (min)	Percentage of pixels deviating more than ±3 SD
80–160	0.7
160–260	1.0
260–380	1.5
380–540	1.4
540–780	1.2

The manufacturer usually only specifies a non-uniformity of less than ±5 per cent. The flood source used was tested by acquiring two flood field images with 90° rotation of the source between measurements. Of the cells within 250 mm diameter, 2.3 per cent were found to deviate more than ±3 SD. The maximum deviation was 2.7 per cent.

Changes in non-uniformity due to rotation of gamma camera. It has been observed that the energy signal from the PM-tubes changes when the camera gantry is rotated (LARSSON). This may be due partly to interaction with magnetic fields, both the earth magnetic field and fields induced by the surrounding electric equipment and partly to gravitational deformation of the dynode structures or changes in the optical transmission from crystal to PM-tube. The magnitude of the energy shift was investigated using point sources directly on the collimator and a multichannel analyser to register the energy signals. Measurements were made with and without individual μ-metal shielding around the PM-tubes. The shields were cylinders covering the en-

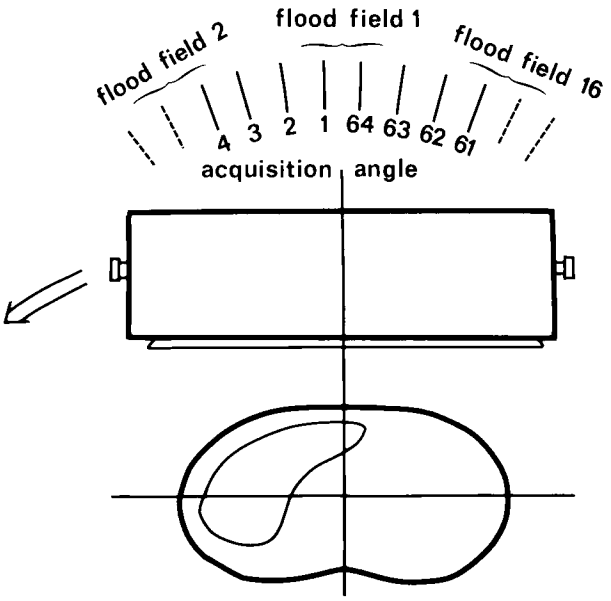

Fig. 8. Non-uniformity correction technique. Flood field 1 is used to correct frame 63–2 in the 64 frame acquisition investigation, flood field 2 to correct frame 3–6, and so on.

tire PM tube. Results obtained with the point source at the center of the gamma camera are presented in Fig. 7. Comparable results were obtained with the point source in other positions. The μ-metal shielding is essential to avoid considerable changes of the energy signal and thus non-uniformity of the field of view during rotation of the camera. It is, however, not obvious that the small energy shift recorded with the μ-metal shields around the PM-tubes will produce noticeable changes of uniformity. This was investigated using a ^{57}Co flood source and 5 cm of polystyrene fixed to the collimator surface. Flood fields were obtained with the camera in angular position 0°, 90°, 180°, 200° and 270°. Approximately 10 000 counts/pixel were accumulated in each angle. All images were compared pixel by pixel to the image obtained with the camera in angular position 180°. The maximum deviation and the number of pixels deviating more than ±3 SD were recorded. The results are presented in Table 3. It can be deduced that rather small areas of the field of view might show substantial changes in count rate depending on angular position of the camera. Similar results have been obtained with other cameras (JAHANGIR et coll. 1982).

The influence of a small energy shift in the PM-tube signal, on non-uniformity, was also analysed from two flood field images, (flood source ^{57}Co +5 cm polystyrene, 10 000 counts/pixel), acquired with an increase of the high tension to the PM-tubes corresponding to 2 keV between acquisitions (measured energy shift when rotating camera max. 2 keV with shields). These flood field images were compared pixel by pixel using the method described. Twelve per cent of the pixels deviated more than ±3 SD. The maximum deviation was 3.8 per cent. The differences in the results obtained when the camera was rotated compared with when the high tension to the PM-tubes was changed depend on that when the camera is rotated, not all PM-tubes are affected in the same way.

Short- and long-term changes of uniformity. Since even very small changes in uniformity will be essential in ECT the stability of the gamma camera as regards uniformity of the field of view should be investigated.

The short-term stability is considered when it is decided what magnitude of uniformity changes that will not indicate the need to acquire a new flood field image. The long-term stability is considered when the periodicity of the uniformity check is decided.

The short-term stability was analysed with a ^{99}Tc^{m} flood source (70 mm thick) and dynamic acquisition. The acquisition time was 20 min per frame for a total of 12 hours. The number of counts/cell × frame was ~3 000 at the beginning. The investigation was divided into 6 different time intervals. The frames within these intervals were added together. The time intervals were chosen so that the average number of counts/pixel were approximately the same in each interval (~12 000 counts/pixel). All images were compared with the image from the first time interval (0–80 min). The number of pixels deviating more than ±3 SD were recorded. The results presented in Table 4 indicate that the short-term changes of uniformity are very small.

The long-term stability was recorded from flood field images (^{57}Co + 5 cm polystyrene) obtained during a time period of ~6 months. During this period the correction matrix for the uniformity corrector was re-acquired twice. It is obvious that the uniformity changed considerably when a new correction matrix was applied. Even without replacement of the correction matrix the changes of uniformity were significant.

Proposed correction technique

The results presented have been used to develop a special non-uniformity correction technique for

ECT. A technique with 16 flood field images acquired in equally spaced angles from 0° to 360° has been tested (Fig. 8). The inverse flood field images are used to correct the acquisition investigation. The correction technique is described in greater detail elsewhere (AXELSSON et coll. 1982). This technique, using flood field images obtained with $^{99}Tc^{m}$ flood source + 5 cm polystyrene and 10000 counts/pixel × angle, was used to correct the phantom experiments presented (Fig. 6). The time needed to correct a 64 angle investigation is approximately 20 s. The images reconstructed after correction of the acquisition investigation are presented in Fig. 9. The sections presented are the same as in Fig. 6. No obvious ring artifacts exist.

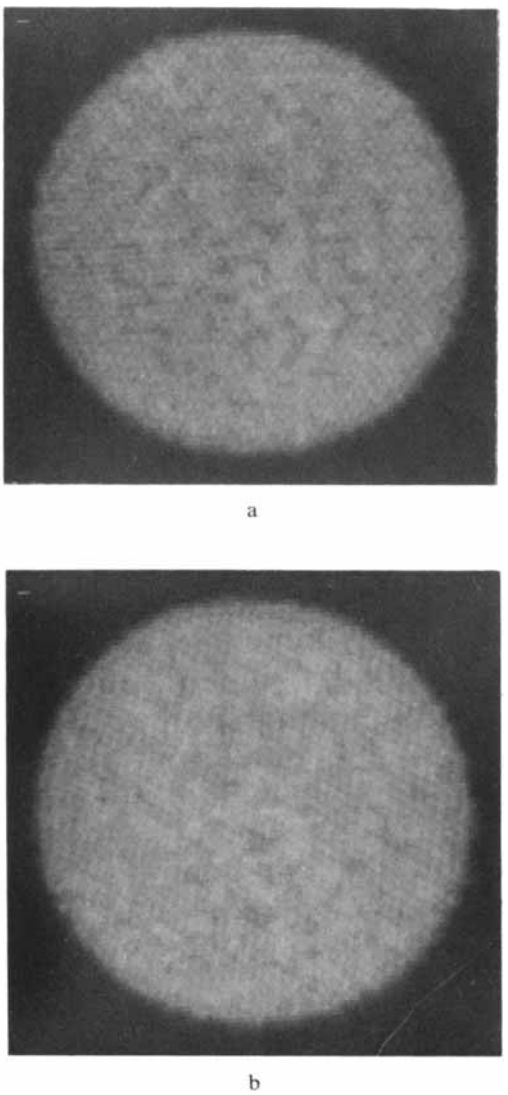

Fig. 9. Images (same sections as in Fig. 6) reconstructed after correction of acquisition with 16 angle correction technique.

Discussion

It is shown that even minor non-uniformity in the field of view of the gamma camera might introduce disturbing artifacts in the reconstructed image. The magnitude of the non-uniformity and thus image artifacts may vary considerably between different gamma cameras partly due to local circumstances. A proper non-uniformity correction technique should be applied to avoid disturbing ring artifacts. The flood field images used should be acquired with scattering material between flood source and collimator and with extremely good statistical accuracy. Care should be taken to account for changes of uniformity during rotation of the camera. Since newly developed gamma cameras have a better stability it might, however, with these cameras, be sufficient to use the same non-uniformity correction matrix for all angles in the acquisition investigation.

The ECT system used has been in clinical use since 1978, mostly for examinations of liver and facial skeleton, but non-uniformity induced artifacts that seriously disturb the reconstructed images have only been observed in a few cases. This is, however, not surprising. In most examinations of the liver neither the liver nor the spleen is close to the center of rotation and thus the artifacts with the largest magnitude are avoided. However, less disturbing artifacts may be present (cf. Fig. 10). The figure presents the same section of the liver reconstructed without correction for non-uniformity (a) and after multiple view non-uniformity correction (b). For example, if the facial skeleton is examined the count density in the central region is only about 30 per cent of the count density in the skull. Since the displayed image normally is normalized to the maximum count density a 20 per cent artifact in the central region will result in a 6 per cent change in the displayed count density. The effect of the non-uniformity correction is thus in most cases not discernible, as is shown by the example in Fig. 10c and d. However, the artifacts degrade the information content of the images without being observed as rings. The effects may, however, be discernible if the images are subject to quantitative evaluation.

In 1978–1979 the system was equipped with a MAXI I (a gamma camera without on-line uniformity correction). Phantom experiments similar to those presented showed less marked ring artifacts than the present system although the level of non-

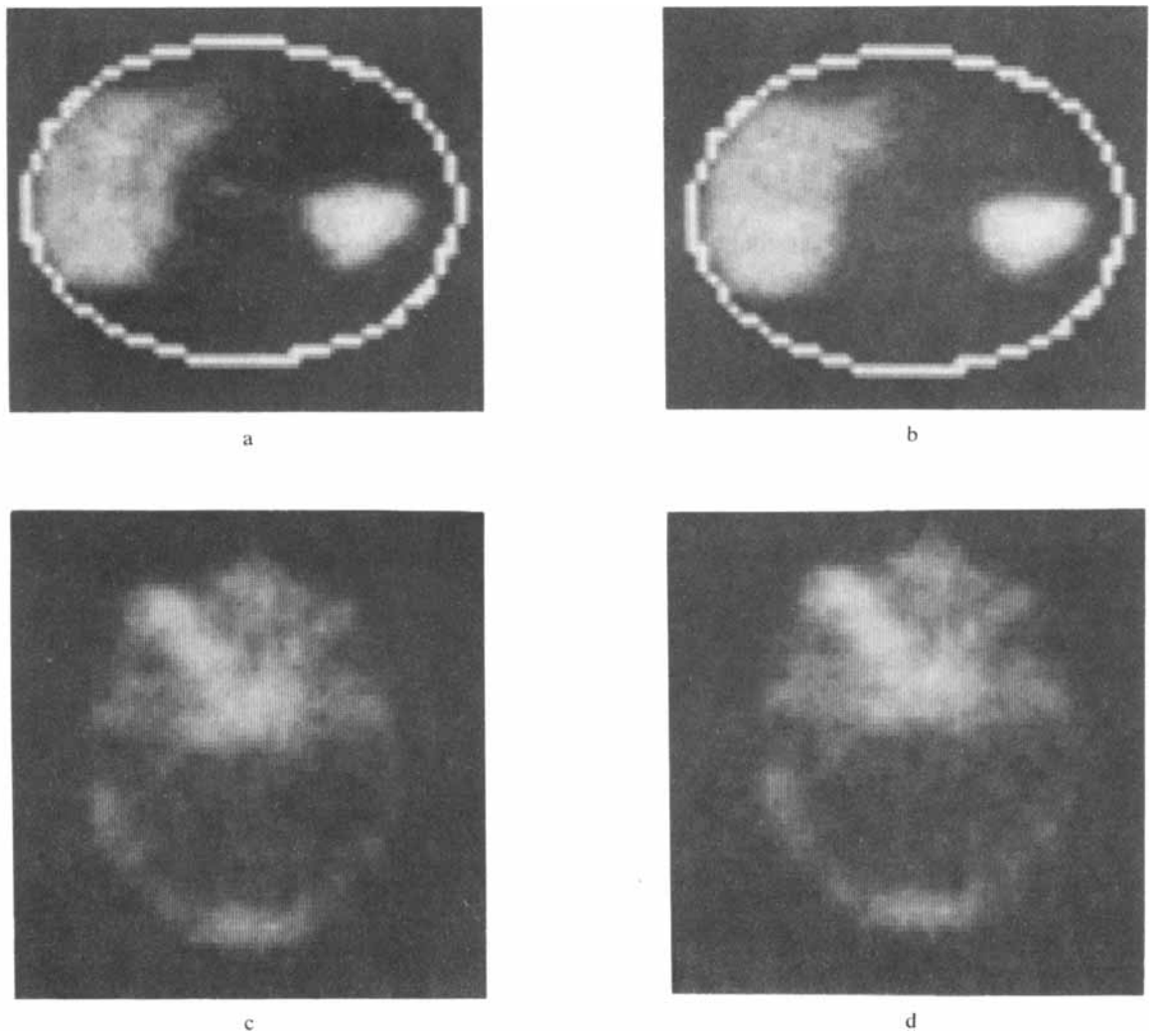

Fig. 10. Investigation of liver (a, b) and facial skeleton (c, d). Images reconstructed without non-uniformity correction (a, c) and after multiple view non-uniformity correction (b, d).

uniformity was about the same. This might be due to more smoothly varying uniformity in MAXI I. Measurements to investigate the magnitude and abundance of non-uniformity artifacts have also been performed on two GE 400T systems with 61 PM-tubes. The measurements and evaluation of the results were done with the technique presented previously. One camera showed results comparable to the 37 PM-tube camera used while the other camera showed somewhat smaller artifacts (maximum artifact amplitude 43% and average rms error within 250 mm diameter 6.2%).

The uniformity must be checked periodically even for very small changes in order to achieve the best results from the non-uniformity correction. The check periodicity should be high until the stability of the system has been confirmed. Since the time to acquire new correction matrices is quite long the tolerance level (maximum tolerable non-uniformity) should be determined in each case. It might be reasonable to have different tolerance levels for the area close to (for example within 5 pixels) the axis of rotation and the peripheral parts of the camera as was discussed for TMT by PARKER et coll. (1982).

SUMMARY

Changes of gamma camera uniformity due to choice of flood source configuration and camera head orientation, and influence of these changes on the reconstructed image, have been analysed using phantom measurements. The transfer of defects in the projection data to the reconstructed image has also been investigated using computer

simulations. The results indicate that the use of gamma cameras for emission computed tomography will impose higher demands on gamma camera uniformity than conventional scintigraphy.

REFERENCES

AXELSSON B., ISRAELSSON A. and LARSSON S.: A method for correction of gamma camera non-uniformity in single-photon emission computed tomography. *In:* Radioaktive Isotope in Klinik und Forschung, Gasteiner Internationales Symposium 1982.

BERGSTEDT H., BONE D., HOLMGREN A., ISRAELSSON A., JOHANSSON B., LAGERGREN C., LARSSON S., LIND M. and LUNDELL G.: Two years clinical experiences of a system for emission computed tomography in gamma camera scintigraphy. XVth International Congress of Radiology, 1981.

BIERSACK H. J., RESKE S. N., KNOPP R. und WINKLER C.: Optimierung der szintigraphischen Diagnostik durch "single-photon" Emissions-Computertomographie. Ergebnisse bei 1300 Patienten. *In:* Radioaktive Isotope in Klinik und Forschung, Gasteiner Internationales Symposium 1982.

COHEN G., KEREIAKES J. G., PADIKAL T. N., ASHARE A. B. and STRENGER E. L.: Quantitative assessment of field uniformity for gamma cameras. Radiology 118 (1976), 197.

GO R. T., COOK S. A., MACINTYRE W. J., UNDERWOOD D., RINCON G., YIANNIKAS J., NAPOLI C. and SALCEDO E.: Comparative accuracy of stress and redistribution Thallium-201 cardiac single-photon emission transaxial tomography and planar imaging in the diagnostic of myocardial ischemia. J. Nucl. Med. 23 (1982), 25.

GULLBERG G. T., NOWAK D. J., EISNER R. L., MALKO J. A. and WORONOWICZ E. M.: A theoretical investigation of non-uniformity errors in rotating gamma camera tomography. J. Nucl. Med. 23 (1982), 53.

HASMAN A. and GROOTHEDDE R. T.: Gamma camera uniformity as a function of energy and count-rate. Brit. J. Radiol. 49 (1976), 718.

JAHANGIR S. M., BRILL A. B., BIZAIS Y. and ROWE R. W.: Count rate variations with detector orientations. J. Nucl. Med. 23 (1982), 45.

KOWALSKI G.: The influence of fixed errors of a detector array on the reconstruction of objects from their projections. IEEE Transactions on Nuclear Science NS 24 (1977), 2006.

LARSSON S.: Gamma camera emission tomography. Acta radiol. (1980) Suppl. No. 363.

LEWIS J. T., NEFF R. A., NISHIGAMA H. and BAHR G. H.: The effect of photon energy on tests of field uniformity in scintillation cameras. J. Nucl. Med. 19 (1978), 553.

MUEHLLEHNER G., WAKE R. H. and SANO R.: Standards for performance measurements in scintillation cameras. J. Nucl. Med. 22 (1981), 72.

NOWAK D. J., GULLBERG G. T., EISNER R. L., MALKO J. A. and WORONOWICZ E. M.: An investigation to determine uniformity requirements for rotating gamma camera tomography. J. Nucl. Med. 23 (1982), 52.

PADIKAL T. N., ASHARE A. B. and KEREIAKES J. G.: Field flood uniformity correction. Benefits or pitfalls? J. Nucl. Med. 17 (1976), 653.

PARKER D. L., COUCH J. L., PESCHMANN K. R., SMITH V., JIMBO M. and WANG E. C.: Design constraints in computed tomography. A theoretical review. Med. Phys. 9 (1982), 531.

PITT W. R. and SHARP P. F.: Reproducibility of gamma camera data. Phys. in Med. Biol. 26 (1981), 693.

ROGERS W. L., CLINTHORNE N. H., HARLENESS B. A., KORAL K. F. and KEYES J. W.: Field-flood requirements for emission computed tomography with an Anger camera. J. Nucl. Med. 23 (1982), 162.

SHEPP L. A. and LOGAN B. F.: The Fourier reconstruction of a head section. IEEE Transaction on Nuclear Science NS 21 (1974), 21.

— and STEIN J. A.: Simulated reconstruction artifacts in computerized X-ray tomography. *In:* Reconstruction tomography in diagnostic radiology and nuclear medicine, p. 33. Edited by M. M. Ter-Pogossian, J. R. Cox, M. E. Phelps, D. O. Davis, G. L. Brownell and R. G. Evans. University Park Press, Baltimore 1977.

SOUSSALINE F. P., TODD-POKROPEK A. E., ZUROWSKI S., HUFFER E., RAYNAUD C. E. and KELLERSOHN C. L.: A rotating conventional gamma camera single-photon tomography system. Physical characterization. J. Ass. Comp. Tomogr. 5 (1981), 551.

TODD-POKROPEK A. E., ERBSMAN F. and SOUSSALINE F. P.: The non-uniformity of imaging devices and its impact in quantitative studies. *In:* Medical radionuclide imaging. Volume 1, p. 67. IAEA, Vienna 1977.

WICKS R. and BLAU M.: Effect of spatial dislocation on Anger camera field-uniformity correction. J. Nucl. Med. 20 (1979), 252.